International Geology Review
Publication details, including instructions for authors and subscription information:
http://www.tandfonline.com/loi/tigr20

He and Ar isotopic compositions and genetic implications for the giant Shizhuyuan W-Sn-Bi-Mo deposit, Hunan Province, South China

Li-Yan Wu [a], Rui-Zhong Hu [a], Jian-Tang Peng [a], Xian-Wu Bi [a], Guo-Hao Jiang [a], Hong-Wei Chen [a], Qiao-Yun Wang [a] & Ya-Ying Liu [a]

[a] State Key Laboratory of Ore Deposit Geochemistry, Institute of Geochemistry, Chinese Academy of Sciences, Guiyang, 550002, PR China

Published online: 23 Feb 2011.

To cite this article: Li-Yan Wu, Rui-Zhong Hu, Jian-Tang Peng, Xian-Wu Bi, Guo-Hao Jiang, Hong-Wei Chen, Qiao-Yun Wang & Ya-Ying Liu (2011) He and Ar isotopic compositions and genetic implications for the giant Shizhuyuan W-Sn-Bi-Mo deposit, Hunan Province, South China, International Geology Review, 53:5-6, 677-690, DOI: 10.1080/00206814.2010.510022

To link to this article: http://dx.doi.org/10.1080/00206814.2010.510022

International Geology Review
Vol. 53, Nos. 5–6, April–May 2011, 677–690

Taylor & Francis
Taylor & Francis Group

He and Ar isotopic compositions and genetic implications for the giant Shizhuyuan W–Sn–Bi–Mo deposit, Hunan Province, South China

Li-Yan Wu, Rui-Zhong Hu*, Jian-Tang Peng, Xian-Wu Bi, Guo-Hao Jiang, Hong-Wei Chen, Qiao-Yun Wang and Ya-Ying Liu

State Key Laboratory of Ore Deposit Geochemistry, Institute of Geochemistry, Chinese Academy of Sciences, Guiyang 550002, PR China

(*Accepted 6 July 2010*)

The Shizhuyuan ore deposit in southern Hunan Province is a world-class W–Sn–Bi–Mo occurrence hosted by Devonian limestone in the thermal aureole of the Qianlishan granite. Mineralization coincided with intrusion of the granite pluton during Mesozoic crustal extension in South China. We present new He and Ar isotope data for volatiles released from pyrite in the Shizhuyuan deposit. Concentrations of ^{40}Ar range from 0.21 to 2.38 $\times 10^{-6}$ cm^3 STP ^{40}Ar/g, and ^4He concentrations range from 0.8 to 65.1 $\times 10^{-6}$ cm^3 STP ^4He/g. $^3He/^4He$ ratios vary from 0.06 to 1.66 *Ra* (where *Ra* is the $^3He/^4He$ ratio of air $= 1.39 \times 10^{-6}$) and $^{40}Ar/^{36}Ar$ ratios range from 293 to 1072. The isotopic compositions of He and Ar indicate that the ore-forming fluids were mantle-derived, modified by air-saturated crustal fluids. Shallow-level boiling increased ^3He concentrations, whereas crustal contamination decreased $^3He/^4He$ ratios in the magmatic fluids. The occurrence of mantle-derived components in the magmatic fluid indicates that the associated Qianlishan granite is not a typical S-type pluton that formed entirely by crustal melting. We propose that the mineralization was related to mantle upwelling and Mesozoic lithosphere extension of the South China Block.

Keywords: He and Ar isotopes; Shizhuyuan W–Sn–Bi–Mo deposit; Qianlishan granite; crust–mantle interaction; Hunan Province, China

Introduction

The Shizhuyuan W–Sn–Bi–Mo deposit, located 15 km SE of Chenzhou City, Hunan Province, China, is one of the largest polymetallic ore deposits in the world. It contains 800,000 tons of tungsten, 500,000 tons of tin, 200,000 tons of bismuth, 100,000 tons of molybdenum, and abundant fluorine (Mao *et al.* 1998). Many researchers have studied the geology (Wang *et al.* 1987; Mao *et al.* 1998), petrogenesis and mineralization (Mao *et al.* 1994; Liu *et al.* 1995; Mao *et al.*1996; Zhao *et al.* 2001), geochronology (Li *et al.* 1996, 2004), and geochemistry (Zhang 1989; Xu *et al*. 2002). However, the origin of the ore-forming fluids is still debated.

He and Ar isotopes are sensitive tracers of volatiles derived from the crust versus the mantle (Ballentine and Burnard 2002a). Simmons *et al.* (1987) successfully used these isotopes to study the origin of hydrothermal fluids in the Casapalca and Pasto Bueno polymetallic deposits, Peru, about three decades ago. Subsequently, numerous similar studies

*Corresponding author. Email: huruizhong@vip.gyig.ac.cn

ISSN 0020-6814 print/ISSN 1938-2839 online

DOI: 10.1080/00206814.2010.510022
http://www.informaworld.com

were published (Stuart *et al.* 1995; Hu *et al.* 1998; Burnard *et al.* 1999; Ballentine *et al.* 2002; Kendrick *et al.* 2002; Burnard and Polya 2004; Hu *et al.* 2004; Li *et al.* 2006; Sun *et al.* 2006). This article presents He and Ar isotopic compositions of volatiles in hydrothermal minerals in the Shizhuyuan W–Sn–Bi–Mo deposit. We use these data to evaluate the origin of the ore-forming fluids.

Geological background

The Shizhuyuan deposit occurs along the northern edge of Dongpo-Yuemei synclinorium, in the South China fold belt of the South China Block. About 30 km NW from the deposit is the prominent Chaling-Linwu deep fault (Figure 1). The deposit covers an area of 1200×600 m^2, with a thickness of 200–300 m. The styles of mineralization (Figure 2) include veinlet Sn–Be ore in marbles (type I), massive W–Sn–Bi–Mo ore in skarn (type II), W–Sn–Bi–Mo–F ore in greisen-stockwork-skarn (type III), and massive W–Sn–Mo–Bi ore in greisen (type IV) (Wang *et al.* 1987; Lu *et al.* 2003). Numerous faults with different strikes transect the area. The NE and NW faults host the stockwork mineralization in the Shizhuyuan mine. The most intense mineralization occurs in deformed skarns and marbles intersected by the major faults.

The sedimentary strata in the ore field include Sinian–Cambrian metasandstone, Middle and Upper Devonian clastic and carbonate rocks, Lower Carboniferous sedimentary rocks, Jurassic and Cretaceous sedimentary rocks. The Middle Devonian was subdivided into the Tiaomajian and Qiziqiao groups, and the Upper Devonian was subdivided into Xikuangshan and Shetianqiao groups. The Devonian Shetianqiao and Qiziqiao groups are most important country rocks (Figure 2). Extensive hydrothermal activity resulted in intensive wall-rock alterations such as skarnization, greisenization, K-feldsparization, albitization, fluoritization, siliconization, and marmarization.

The Shizhuyuan polymetallic deposit occurs in the contact zone between the Qianlishan granite and the Devonian limestone. The Yanshanian Qianlishan granite pluton ($\sim$10 km^2) is composed of three intrusive phases: pseudoporphyritic biotite granite, equigranular biotite granite, and granite porphyry (Mao and Li 1995). Strong alteration of skarn and greisen that formed in the contact zone between the first and second phases of granite intrusions and Devonian limestone is responsible for the polymetallic mineralization. The igneous rocks have zircon SHRIMP U–Pb ages of 152 ± 2 million years (Li *et al.* 2004). The age of mineralization varies from 151 ± 3.5 (Re–Os isochron; Li *et al.* 1996), 149 ± 2 (Sm–Nd isochron; Li *et al.* 2004) to 148.2 ± 1.1 million years (mica ^{40}Ar–^{36}Ar; Peng *et al.* 2006), similar to the age of the Qianlishan granite. For decades, the Qianlishan granite has been regarded as the product of crustal remelting and thus classified as of S-type (Xu *et al.* 1984; Wang *et al.* 1987; Zhang 1989). However, the occurrence of abundant mafic microgranular enclaves (MME) in the granite (Ma *et al.* 2005) and the low initial ^{87}Sr/^{86}Sr ratios of the pluton (0.703–0.729) suggest mixing between crust- and mantle-derived materials (Zhao *et al.* 2001).

Fluid inclusions in quartz associated with mineralization are dominantly small (5–20 μm in diameter; Figure 3), with low to high salinity (1.2–32.0 wt.% NaCl eq.) and homogenization temperatures of 156–450°C. Fluid inclusion data suggest that at least two types of fluids were associated with mineralization: one with high salinity and a high homogenization temperature, and the other with low salinity and a low homogenization temperature. The occurrence of coexisting saline fluid and vapour inclusions suggests boiling during mineralization (Figure 3).

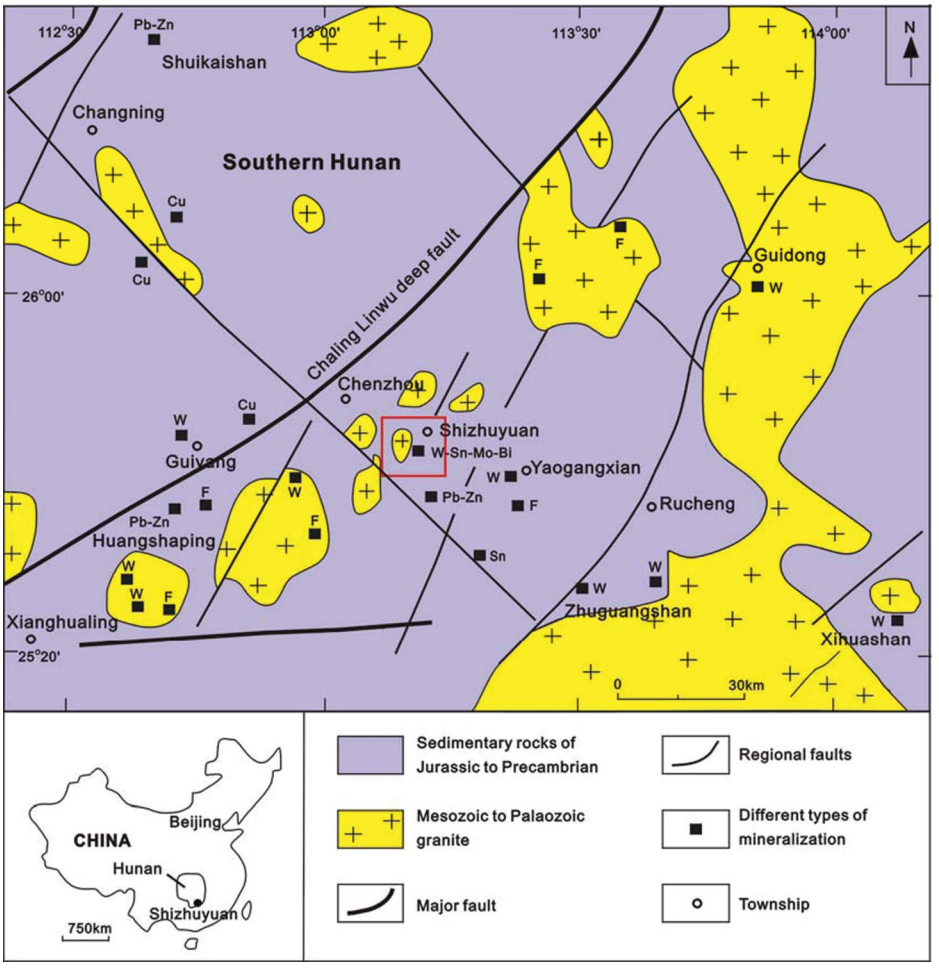

Figure 1. Regional geologic map of southern Hunan Province, China (after Lu *et al.* 2003).

Sampling and experimental methods

All pyrite samples used in this study were collected from the underground mining cuts at the levels of 358, 490, 536, and 620 m in the Shizhuyuan mine. They are from three types of ore: W–Bi–Mo–Sn massive skarn ore (type II), W–Sn–Mo–Bi–F stockwork ore (type III), and W–Sn–Mo–Bi massive greisen (type IV). In these samples, pyrite occurs as vein or mesh-vein structure, massive aggregates, and disseminated assemblages (Figure 4). All pyrite crystals selected for this study are not deformed, with grain sizes varying from 0.1 to 5 mm in diameter.

The samples were first crushed and then hand-picked under a binocular microscope. He and Ar isotopic compositions of volatiles released from the samples were measured with a VG 5400 inert gas mass spectrometer at the State Key Laboratory of Ore Deposit Geochemistry, Institute of Geochemistry, Chinese Academy of Sciences. The mass spectrometer was regularly calibrated against 1.32×10^{-7} cm^3 STP Ar with air $^{40}Ar/^{36}Ar$, and 5.6×10^{-7} cm^3 STP He with $^3He/^4He = 1.4 \times 10^{-6}$. The volatile extraction and analytical procedures are similar to those of Stuart *et al.* (1994a). The pyrite samples were

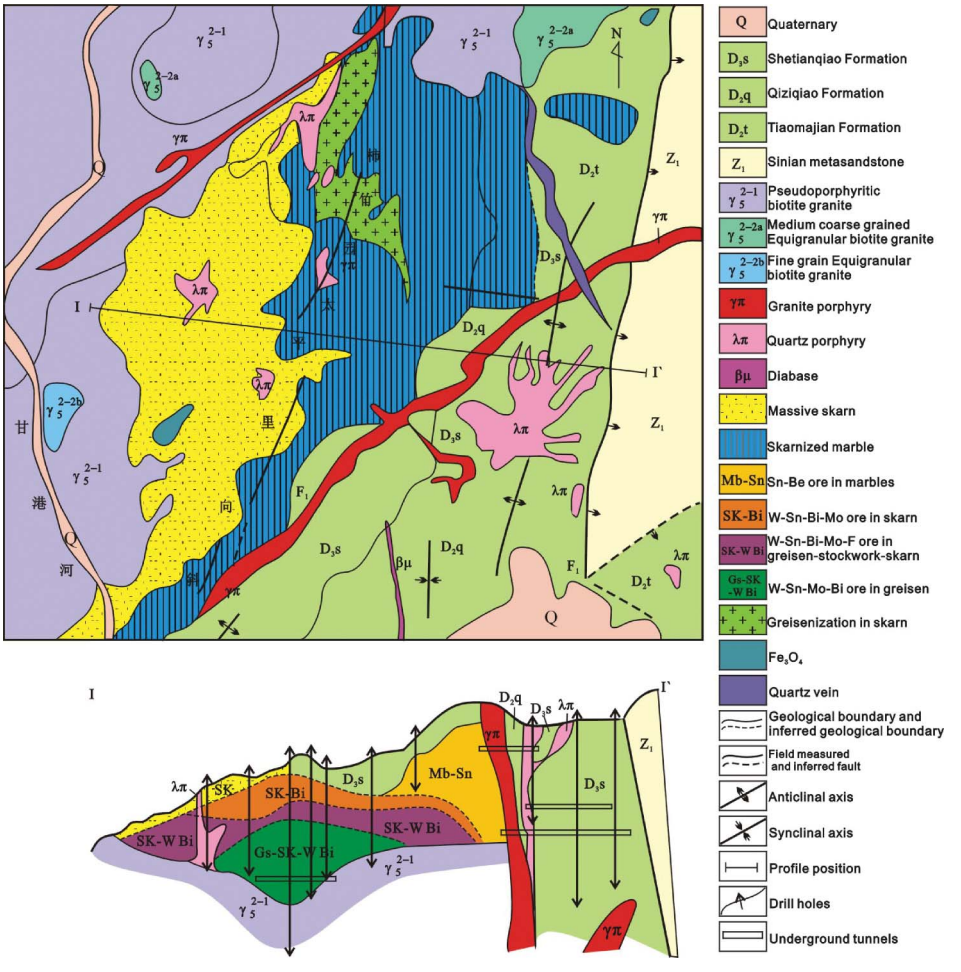

Figure 2. Geological and profile map of the Shizhuyuan deposit (modified from Zhao 2004).

ultrasonically cleaned with acetone for 20 min before loading into the online in vacuo crushing devices. Approximately 0.5–1 g of sample was loaded into a screw-type crusher. The samples were heated at 120–150°C in vacuum for 24 h to remove adhered atmospheric contaminants. The samples were then crushed to release volatiles from fluid inclusions in pyrite. The released gases were purified to remove reactive gas species. Ar and Xe were kept in a cold trap whereas He and Ne were released to the online analytical system. Ar was released at −78°C for isotope determination.

Results

The noble gas compositions of volatiles released from pyrite crystals from the Shizhuyuan deposit are listed in Table 1 and Figure 5. The concentrations of ^{40}Ar range from 0.21 to 2.38 × 10^{-6} cm^3 STP ^{40}Ar/g, and ^{4}He concentrations are 0.8–65.1 × 10^{-6} cm^3 STP ^{4}He/g. The large variations in the noble gas isotopic concentrations may reflect variable fluid inclusion abundance in the sample. The ^{3}He/^{4}He ratios vary from 0.06 to 1.66 *Ra* (*Ra* represents the ^{3}He/^{4}He ratio of air, 1.39 × 10^{-6}). The ^{40}Ar/^{36}Ar ratios vary between 293 and 1072.

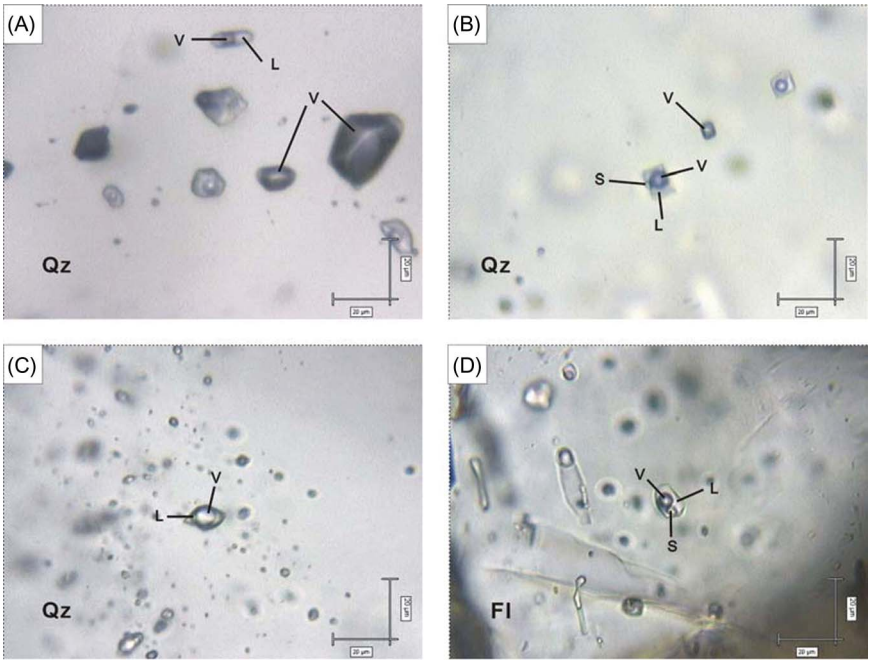

Figure 3. Fluid inclusions in quartz and fluorite in the Shizhuyuan deposit. (A) Vapour-rich and aqueous inclusions in quartz (sample SZY-490-4, level 490 m). (B) Daughter mineral-bearing and vapour-rich inclusions in quartz (sample SZY-385-2, level 385 m). (C) CO_2-rich inclusions in quartz (sample SZY-490-III-4, level 490 m). (D) Daughter mineral-bearing fluid inclusions in fluorite (sample SZY-114, level 385 m). Abbreviations: qz = quartz, fl = fluorite, L = liquid, v = vapour, S = daughter mineral.

Discussion

Pyrite is known to be a suitable trap for noble gases (Stuart *et al.* 1994b; Baptiste and Fouquet 1996; Hu *et al.* 1998; Burnard *et al.* 1999). Inclusion-trapped He and Ar are unlikely to be extensively lost within 100 million years (Burnard *et al.* 1999). Even though the trapped He and Ar are partially lost, the ratios of $^{3}He/^{4}He$ and $^{40}Ar/^{36}Ar$ can still remain unchanged (Baptiste and Fouquet 1996; Hu *et al.* 1997; Ballentine and Burnard 2002b; Hu *et al.* 2004). Because the pyrite samples used in this study are from underground workings, cosmogenic ^{3}He can be ruled out (Simmons *et al.* 1987; Stuart *et al.* 1995). The measured He is not the product of nuclear decay of lithium because pyrite is not a Li-bearing mineral (Ballentine and Burnard 2002b). The in situ produced ^{40}Ar from mineral lattice and fluid inclusions are thought to be negligible due to low diffusivity of Ar in pyrite (York *et al.* 1982; Smith *et al.* 2001) and the extremely low K concentration in pyrite (York *et al.* 1982). The amount of radiogenic ^{4}He produced from the decay of U and Th is within the analytical errors. In addition, the fluid inclusions in quartz and fluorite coexisting with pyrite are all primary (Figure 3). Therefore, the measured values of He and Ar abundances and isotopic compositions of the pyrite samples likely represent the characteristics of primary fluid inclusions of ore-forming fluids of the deposit.

Hydrothermal fluids contain noble gases from three ultimate sources (Burnard *et al.* 1999; Ballentine *et al.* 2002): (1) air-saturated (i.e. meteoric) water; (2) mantle-derived fluids; and (3) He and Ar produced in the crust. Air-saturated water has He and Ar isotopic

compositions of $^{3}He/^{4}He = 1.39 \times 10^{-6}$ (1 *Ra*), and $^{40}Ar/^{36}Ar = 295.5$, similar to the atmosphere values, because air-saturated water is isotopically in equilibrium with the atmosphere. The upper oceanic mantle has $^{3}He/^{4}He$ ratio of $1–1.3 \times 10^{-5}$ (7–9 *Ra*), and the subcontinental lithospheric mantle (SCLM) has $^{3}He/^{4}He$ ratio of $0.8–1 \times 10^{-5}$ (6–7 *Ra*) (Porcelli *et al.* 1992; Patterson *et al.* 1994; Dunai and Baur 1995; Reid and Graham 1996; Gautheron and Moreira 2002). Mantle-derived Ar has $^{40}Ar/^{36}Ar$ ratios >40,000. Crustal lithophile elements can produce abundant radiogenic and nucleogenic Ar and He. As a result, fluids reacted with crustal rocks will eventually have He and Ar isotopic compositions similar to that of the crust that has $^{40}Ar/^{36}Ar$ ratios ≥1000 (Drescher *et al.* 1998) and $^{3}He/^{4}He$ ratios of 0.01–0.05 *Ra* (Tolstikhin 1978; Stuart *et al.* 1995).

The proportion of atmospheric He can be calculated using the $F^{4}He$ values, which are defined as the $^{4}He/^{36}Ar$ ratio of the sample relative to the atmospheric $^{4}He/^{36}Ar$ value of 0.1655. A sample containing 100% atmospheric He will have an *F* value of unity. The $F^{4}He$ values for all the samples studied by us are much greater than 1 (Table 1), indicating that the volatiles released from pyrite contain negligible atmospheric He. Mantle-derived He and radiogenic He produced in the crust are more important in our samples (Turner *et al.* 1993). As shown in Figure 3, the $^{3}He/^{4}He$ ratios of the volatiles released from pyrite crystals of the Shizhuyuan deposit are similar to or higher than the crust values but lower than the subcontinental mantle values, indicating that the volatiles are dominated significantly by crustal-derived fluid with minor mantle-derived fluid. The correlation between He and Ar isotopic compositions (Figures 6 and 7) indicates mixing between two fluids, one with

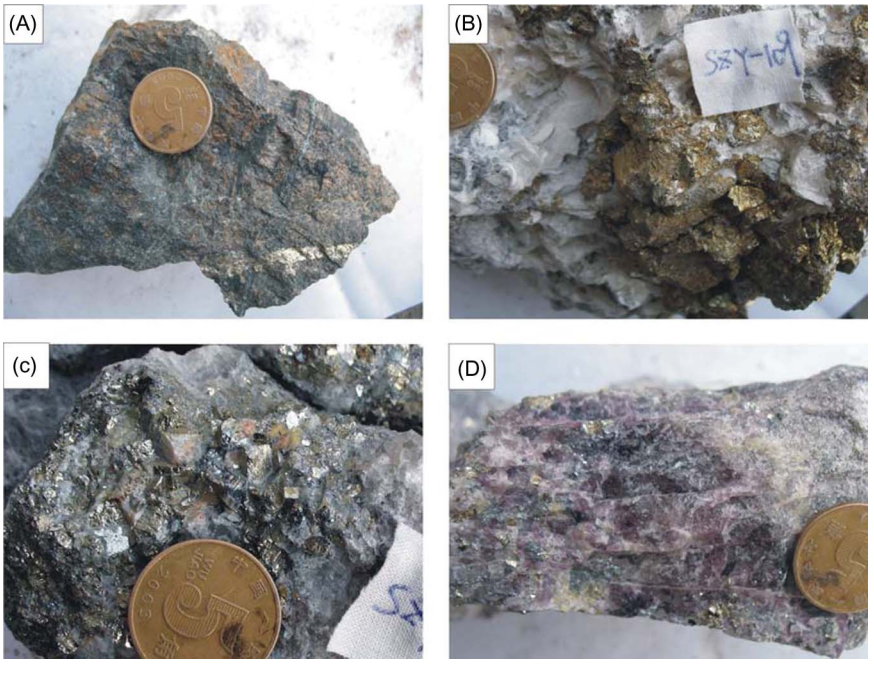

Figure 4. Photographs of the Shizhuyuan pyrite samples. (A) Pyrite occurs as a small veinlet in massive skarn. (B) Massive pyrite in greisen. (C) Cubic pyrite associated with colourless fluorite and bismuthinite. (D) Disseminated pyrite and bismuthinite associated with violet fluorite.

Table 1. He and Ar isotopic compositions of volatiles released from pyrite in the Shizhuyuan deposit.

Sample	Sampling location	Mineralization type	Sample description	Mineral
SZY-9	490 underground tunnel	III	Pyrite vein in greisen-stockwork-skarn	Pyrite
SZY-22	490 underground tunnel	IV	Pyrite vein in silicious rock	Pyrite
SZY-83	620 underground tunnel	II	Pyrite veinlet in massive skarn	Pyrite
SZY-89	620 underground tunnel	III	Massive pyrite associated with pyrrhotine	Pyrite
SZY-90	620 underground tunnel	III	Pyrite vein in greisen-stockwork-skarn	Pyrite
SZY-105	536 underground tunnel	III	Disseminated pyrite associated with bismuthinite in colourless fluorite-stockwork	Pyrite
SZY-107	536 underground tunnel	III	Massive pyrite with fluorite veinlets	Pyrite
SZY-108	536 underground tunnel	III	Disseminated pyrite associated with bismuthinite in violet fluorite-stockwork	Pyrite
SZY-109	536 underground tunnel	IV	Massive pyrite associated with sheeted muscovite and quartz	Pyrite
SZY-112	385 underground tunnel	III	Pyrite veinlet in quartz vein	Pyrite
SZY-113	385 underground tunnel	III	Pyrite veinlet in quartz vein	Pyrite
SZY-120	385 underground tunnel	IV	Disseminated pyrite in greisen	Pyrite
SZY-127	385 underground tunnel	III	Pyrite veinlet in quartz vein	Pyrite

Weight[a] (g)	$^{4}He^{b}$ ($cm^{3}STP$)	$^{40}Ar^{b}$ ($cm^{3}STP$)	$^{3}He/^{4}He$ (Ra)	$^{38}Ar/^{36}Ar$	$^{40}Ar/^{36}Ar$	$^{40}Ar^{*}/^{4}He^{c}$
0.3138	5.34×10^{-7}	1.78×10^{-7}	0.378 ± 0.005	0.195 ± 0.007	365.4 ± 4	0.064
0.411	1.52×10^{-6}	2.28×10^{-7}	0.579 ± 0.003	0.190 ± 0.006	448.5 ± 7	0.051
0.2578	1.07×10^{-6}	6.13×10^{-7}	0.449 ± 0.009	0.187 ± 0.004	349.6 ± 1	0.089
0.2465	7.55×10^{-7}	3.34×10^{-7}	0.171 ± 0.005	0.184 ± 0.003	322.8 ± 1	0.037
0.2222	4.92×10^{-7}	n[d]	0.306 ± 0.004			
0.3545	2.62×10^{-6}	1.86×10^{-7}	0.280 ± 0.004	0.193 ± 0.013	527.7 ± 7	0.035
0.3474	2.26×10^{-5}	7.14×10^{-8}	0.063 ± 0.003	0.118 ± 0.027	785.0 ± 33	0.002
0.4159	1.47×10^{-5}	7.42×10^{-7}	0.143 ± 0.003	0.187 ± 0.0007	311.9 ± 1	0.003
0.34	1.09×10^{-6}	1.16×10^{-7}	1.662 ± 0.009	0.186 ± 0.019	1071.8 ± 48	0.084
0.2182	1.83×10^{-7}	3.56×10^{-7}	0.517 ± 0.009	0.186 ± 0.005	287.8 ± 1	0.015
0.2414	5.20×10^{-7}	4.71×10^{-7}	0.459 ± 0.004	0.182 ± 0.003	317.8 ± 1	0.063
0.2543	2.16×10^{-7}	3.51×10^{-7}	0.704 ± 0.007	0.186 ± 0.002	294.4 ± 2	
0.2077	1.68×10^{-7}	3.62×10^{-7}	0.428 ± 0.01	0.184 ± 0.001	292.8 ± 1	

^{4}He ($cm^3STP \cdot g^{-1}$)	^{40}Ar ($cm^3STP \cdot g^{-1}$)	F^{4}He
1.7027×10^{-6}	5.6594×10^{-7}	6590
3.7003×10^{-6}	5.5418×10^{-7}	18069
4.1321×10^{-6}	2.3765×10^{-6}	3667
3.061×10^{-6}	1.3547×10^{-6}	4414
2.2156×10^{-6}		
7.3776×10^{-6}	5.2358×10^{-7}	48449
6.5104×10^{-5}	2.0561×10^{-7}	1498044
3.536×10^{-5}	1.7837×10^{-6}	37340
3.2143×10^{-6}	3.4195×10^{-7}	56039
8.3736×10^{-7}	1.6335×10^{-6}	921
2.155×10^{-6}	1.9498×10^{-6}	2126
8.5127×10^{-7}	1.3817×10^{-6}	1078
8.0739×10^{-7}	1.7427×10^{-6}	812

Notes: [a]Sample weights are the fraction of crushed pyrite that passes through a 100-μm diameter sieve. [b]Uncertainties in noble gas concentrations are ≈5%; quoted errors of isotope ratios are for 1σ. [c]^{40}Ar* refers to the excess Ar. [d]Not analysed.

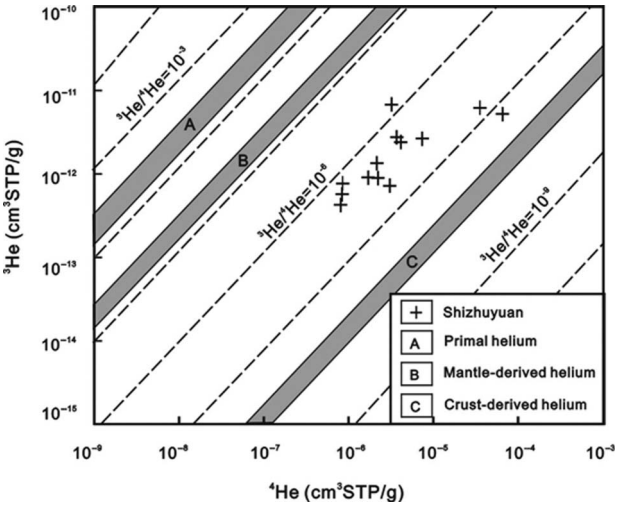

Figure 5. Helium isotopes of volatiles released from pyrite in the Shizhuyuan W–Sn–Bi–Mo deposit. (A), (B), and (C) are from Mamyin and Tolstikhin (1984).

high ^{3}He/^{4}He, high ^{40}Ar/^{36}Ar and the other with low ^{3}He/^{4}He and near-atmospheric ^{40}Ar/^{36}Ar. This is consistent with the presence of two types of fluid inclusions in quartz in the deposit. One type of fluid inclusions has salinity from 26 to 41 wt.% NaCl eq., and the other has salinity from 1 to 21 wt.% NaCl eq. (Lu *et al.* 2003). The high ^{3}He/^{4}He, high ^{40}Ar/^{36}Ar fluid was most likely derived from a magmatic source whereas the low ^{3}He/^{4}He, near-atmospheric ^{40}Ar/^{36}Ar fluid was undoubtedly surface-derived or 'modified air-saturated water' (MASW).

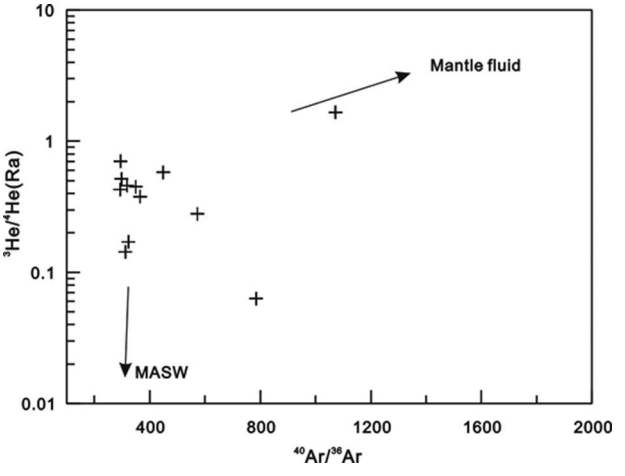

Figure 6. Plot of $^{40}Ar/^{36}Ar$ versus $^{3}He/^{4}He$ except the sample SZY-107, a remarkable mixing line exists for two fluids.

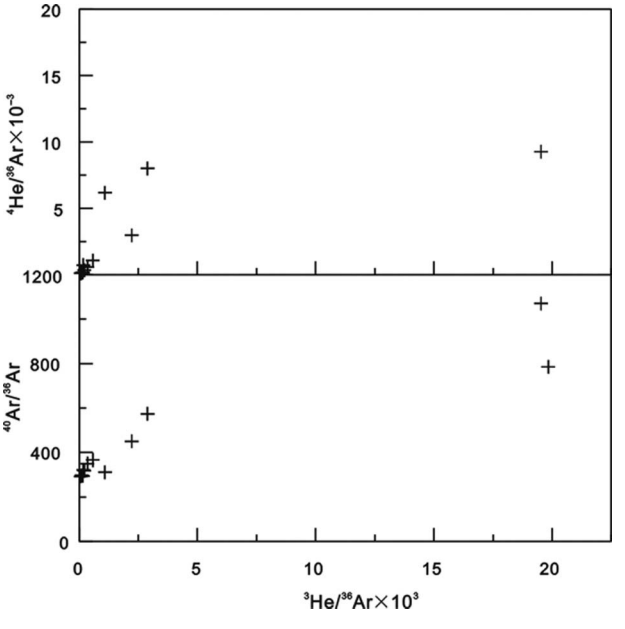

Figure 7. Plots of $^{3}He/^{36}Ar$ versus $^{4}He/^{36}Ar$(top) and $^{3}He/^{36}Ar$ versus $^{40}Ar/^{36}Ar$ (bottom). Least-square fitting to the data gives the equations: $^{4}He/^{36}Ar = (8.21 \times 10^{5})\ ^{3}He/^{36}Ar+1311$, $r^2 = 0.72$; $^{40}Ar/^{36}Ar = (3.09 \times 10^{4})\ ^{3}He/^{36}Ar+330.87$, $r^2 = 0.88$.

Modified air-saturated water

The crustal component in the volatiles released from pyrite crystals probably contains radiogenic ^{4}He and (to a lesser extent) radiogenic ^{40}Ar. In contrast, the $^{3}He/^{36}Ar$ of the MASW is unlikely to be changed because both ^{3}He and ^{36}Ar are not radiogenic. Therefore, it is possible to estimate the $^{40}Ar/^{36}Ar$ for the MASW endmember by extrapolating the trends in Figure 7 to the $^{3}He/^{36}Ar$ value of PASW (pure air-saturated water, 5×10^{8}; Hu

et al. 2004). The estimated $^{40}Ar/^{36}Ar$ for the MASW endmember is 331, which is close to the Ar isotopic composition of PASW ($^{40}Ar/^{36}Ar \approx 295.5$, Turner *et al.* 1993; Stuart *et al.* 1995; Burnard *et al.* 1999) plus minor radiogenic ^{40}Ar derived either from crustal rocks (Stuart *et al.* 1995) or from ^{40}Ar produced by in situ decay of ^{40}K. Similarly, the $^{3}He/^{4}He$ for the MASW endmember is estimated to be 0.08 Ra by extrapolating the trends in Figure 8 to $^{40}Ar^*/^{4}He$ value of 0. This value is much lower than the value of PASW ($^{3}He/^{4}He = 1$ *Ra*), but close to the crustal value, indicating the presence of radiogenic ^{4}He derived from crustal rocks or from ^{4}He produced by in situ decay of U and Th.

A $^{40}Ar^*/^{4}He$ ratio of 0.1 is obtained from the correlation (albeit poor) between $^{3}He/^{4}He$ and $^{40}Ar^*/^{4}He$ (Figure 8), similar to but slightly lower than the estimated value for the crust (≈ 0.2) (Torgersen *et al.* 1989; Ballentine and Burnard 2002b). The low $^{40}Ar^*/^{4}He$ ratios of MASW are attributed to preferential acquisition of ^{4}He over ^{40}Ar from aquifer rocks (Torgersen *et al.* 1989), due to the higher closure temperature of Ar relative to He (Torgersen *et al.* 1989; Ballentine and Burnard 2002b). Ar is quantitatively retained in most minerals at 250°C, whereas the closure temperature of He is usually less than 200°C (Lippolt and Weigel 1988; McDdougall and Harrison 1988; Elliot *et al.* 1993). The MASW trapped in these samples acquired not only He but also Ar from crustal rocks, implying that it was a relatively high-temperature fluid ($\geq$200°C), which is consistent with the homogenization temperatures (156–450°C) of fluid inclusions in coexisting quartz.

The proportion of $^{40}Ar^*$ can be estimated by the measured $^{40}Ar/^{36}Ar$ values according to the following equation (Kendrick *et al.* 2001):

$$^{40}Ar^*\% = \frac{(^{40}Ar/^{36}Ar)_{sample} - 295.5}{(^{40}Ar/^{36}Ar)_{sample}} \times 100$$

The estimated concentrations of $^{40}Ar^*$ range from 0.2 to 72.4%, and the proportion of air-derived ^{40}Ar is as high as 27.6–99.8% (72.6% average).

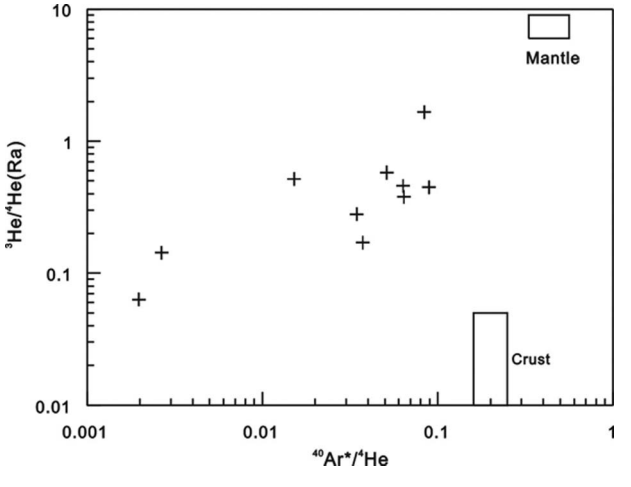

Figure 8. Plot of $^{40}Ar^*/^{4}He$ versus R/Ra. Least square fitting to the data gives the equation: $^{3}He/^{4}He = 8.7856 \times {}^{40}Ar^*/^{4}He + 0.0805$, $r^2 = 0.37$.

Magmatic fluid

High $^{40}Ar/^{36}Ar$ ratios and high ^{3}He values are unique for the mantle (Stuart *et al.* 1995). Therefore, the inferred endmember with high $^{40}Ar/^{36}Ar$ and high ^{3}He (Figure 6) is most likely mantle derived. Using a value of 6 Ra to represent the mantle He, and 0.03 Ra for crustal fluid, the proportion of mantle He is estimated to be between 0.6 and 27.3% (mainly in the range of 1–10%), indicating a small quantity of mantle-derived fluid in our samples.

The concentrations of ^{3}He in our samples are extremely high ($0.4–6.8 \times 10^{-12}$ cm^3 STP g^{-1}), higher than in basaltic phenocrysts and most xenoliths in basalts, but lower than in some basaltic glasses (Burnard and Polya 2004). The concentration of ^{3}He in the fluid ($[^{3}He]_{fluid}$) may be estimated by assuming that the measured ^{36}Ar is entirely derived from air-saturated water. The $^{3}He/^{36}Ar$ ratios of our samples are in the range 0.0001–0.0198, corresponding $[^{3}He]_{fluid}$ from 5.4×10^{-12} to 1.5×10^{-8} cc STP g^{-1} H_2O assuming $[^{36}Ar]_{fluid} = 7.65 \times 10^{-7}$ cc STP g^{-1} H_2O. The estimated $[^{3}He]_{fluid}$ values are very high, which may have resulted from boiling and selective sampling of the vapour phase (Ballentine *et al.* 2002). The characteristics of fluid inclusions in coexisting quartz suggest that boiling may have indeed occurred during mineralization.

The $^{3}He/^{4}He$ ratio of mantle-derived fluid is estimated to be 2.28 Ra by extrapolating the trend in Figure 8 to the $^{40}Ar^{*}/^{4}He$ ratio of 0.25. The estimated value is much lower than that of the subcontinental lithospheric mantle. This probably resulted from crustal anatexis due to underplating of mantle-derived magma or addition of radiogenic ^{4}He produced by decay of U and Th. However, assuming U 2.7×10^{-6} (which is possibly much higher than the true value), Th/U = 0 (Th solubility in hydrothermal fluid is extremely low), and age of 160 million years, the amount of radiogenic ^{4}He ingrowth is within the analytical uncertainty. Therefore, the low $^{3}He/^{4}He$ ratio in the mantle-derived fluid endmember most probably resulted from mixing between mantle-derived magma and melts produced by crustal anatexis.

Genetic implications

The ore-forming fluids of the Shizhuyuan deposit are thought to be mainly derived from the Qianlishan granitic magma (Zhang 1989; Xu *et al.* 2002). Our He and Ar isotopes show that mantle-derived fluid is present in the volatiles trapped in pyrite in the contact zone of the granite, suggesting mantle-derived materials were involved in the formation of the Qianlishan granite pluton. This is consistent with Sr isotopes ($^{87}Sr/^{86}Sr = 0.703–0.729$, Mao *et al.* 1995) of the Qianlishan granite pluton. In addition, the studies of MME in the Middle–Late Jurassic granite in the middle segment of the Nanling Mountains also show that the Qianlishan granite is formed by crust–mantle interaction (Ma *et al.* 2005). Therefore, we do not believe that the Qianlishan granite is typical S-type.

The origin of the Qianlishan granite pluton and the Shizhuyuan deposit is most likely related to mantle upwelling and lithospheric extension in South China during the Mesozoic. Mantle-derived magma ascended to mid-lower crust, providing heating and inducing crustal anatexis. Mixing between them formed hybrid magma. Such hybrid magma continued to ascend to shallow crust at levels and continued to provide heating. The emplacement of the hybrid magma triggered large-scale fluid convection in the region, producing mineralization along the contact zones as well as in the nearly fault systems. Similar condition was made previously by Li *et al.* (2006) who studied the Furong Sn ore deposit in the region.

Conclusions

(1) $^{3}He/^{4}He$ and $^{40}Ar/^{36}Ar$ ratios of volatiles released from pyrite in the Shizhuyuan W–Sn–Bi–Mo polymetallic deposit range from 0.06 to 1.66 *Ra* and from 293 to 1072, respectively. The measured He and Ar isotopic compositions of the fluid inclusion samples are considered to represent the primary ore-forming fluids.

(2) We infer that the ore-forming fluids in the Shizhuyuan deposit formed by mixing of high $^{3}He/^{4}He$ and high $^{40}Ar/^{36}Ar$ magmatic fluid, and low $^{3}He/^{4}He$ and low $^{40}Ar/^{36}Ar$ meteoric water. The meteoric water experienced an intensive interaction with crustal rocks, gaining crustal He and near-atmospheric Ar isotopic signatures. The magmatic fluid was contaminated by MASW with crustal $^{3}He/^{4}He$ and near-atmospheric $^{40}Ar/^{36}Ar$. The magmatic fluid was derived from the Qianlishan granite pluton. This igneous body has He and Ar isotopes consistent with mantle derivation as well as a crustal melt. This suggests that the Qianlishan granite is not a typical S-type pluton. We conclude that the pluton and the associated Shizhuyuan deposit are related to mantle upwelling and lithospheric extension in South China during Mesozoic time.

Acknowledgements

We are grateful to Prof. Pete Burnard and Dr Mark Kendrick for their comments on the early version of the manuscript and to Prof. Chusi Li for his useful suggestions for improving the manuscript. We thank the geologists of the Shizhuyuan Mine for their field assistance. This research was supported jointly by the National Natural Science Foundation of China (40903023), the Major Programme of the National Natural Science Foundation of China (40634020), and the National Basic Research Development Programme of China (973 Programme) (2007CB411408; 2007CB411408).

References

Ballentine, C.J., Burgess, R., and Marty, B., 2002, Tracing fluid origin, transport and interaction in the crust: Reviews in Mineralogy and Geochemistry, v. 47, no. 1, p. 539–614.

Ballentine, C.J., and Burnard, P.G., 2002a, Noble gases in the continental crust, *in* Porcelli, D.R., Ballentine, C.J., and Wieller, R. eds., Noble Gases in Geochemistry and Cosmochemistry: Reviews in Mineralogy and Geochemistry, volume 47, p. 482–536.

Ballentine, C.J., and Burnard, P.G., 2002b, Production, release and transport of noble gases in the continental crust: Reviews in Mineralogy and Geochemistry, v. 47, no. 1, p. 481–538.

Baptiste, P.J., and Fouquet, Y., 1996, Abundance and isotopic composition of helium in hydrothermal sulfides from the East Pacific Rise at 13° N: Geochimica et Cosmochimica Acta, v. 60, no. 1, p. 87–93.

Burnard, P.G., Hu, R.Z., Turner, G., and Bi, X.W., 1999, Mantle, crustal and atmospheric noble gases in Ailaoshan gold deposits, Yunnan province, China: Geochimica et Cosmochimica Acta, v. 63, no. 10, p. 1595–1604.

Burnard, P.G., and Polya, D.A., 2004, Importance of mantle-derived fluids during granite associated hydrothermal circulation: He and Ar isotopes of ore minerals from Panasqueira: Geochimica et Cosmochimica Acta, v. 68, no. 7, p. 1607–1615.

Drescher, J., Kirsten, T., and Schäfer, K., 1998., The rare gas inventory of the continental crust, recovered by the KTB continental deep drilling project: Earth and Planetary Science Letters, v. 154, no. 1–4, p. 247–263.

Dunai, T.J., and Baur, H., 1995, Helium, neon and argon systematics of the European subcontinental mantle: Implications for its geochemical evolution: Geochimica et Cosmochimica Acta, v. 59, no. 13, p. 2767–2784.

Elliot, T., Ballentine, C.J., O'Nions, R.K., and Ricchiuto, T., 1993, Carbon, helium, neon and argon isotopes in a Po basin naturalgas field: Chemical Geology, v. 106, no. 3–4, p. 429–440.
Gautheron, C., and Moreira, M., 2002, Helium signature of the subcontinental lithospheric mantle: Earth and Planetary Science Letters, v. 199, no. 1–2, p. 39–47.
Hu, R.Z, Bi, X.W., Shao, S.X., Turner, G., and Burnard, P.G., 1997, Helium isotopic compositions in the Machangqing copper deposit Yunnan Province: Chinese Science Bulletin, v. 42, no. 17, p. 1542–1545 (in Chinese).
Hu, R.Z., Burnard, P.G., Bi, X.W., Zhou, M.F., Peng, J.T., Su, W.C., and Wu, K.X., 2004, Helium and argon isotope geochemistry of alkaline intrusion-associated gold and copper deposits along the Red River-Jinshajiang fault belt, SW China: Chemical Geology, v. 203, no. 3–4, p. 305–317.
Hu, R.Z., Burnard, P.G., Turner, G., and Bi, X.W., 1998, Helium and argon isotope systematics in fluid inclusions of Machangqing copper deposit in West Yunnan Province, China: Chemical Geology, v. 146, no. 1–2, p. 55–63.
Kendrick, M.A., Burgess, R., Pattrick, R.A., and Turner, G., 2001, Fluid inclusion noble gas and halogen evidence on the origin of Cu-porphyry mineralizing fluids: Geochimica et Cosmochimica Acta, v. 65, no. 16, p. 2651–2668.
Kendrick, M.A., Burgess, R., Pattrick, R.A., and Turner, G., 2002, Hydrothermal fluid origins in a fluorite-rich Mississippi valley-type district; combined noble gas (He, Ar, Kr) and halogen (Cl, Br, I) analysis of fluid inclusions from the South Pennine ore field, United Kingdom: Economic Geology, v. 97, no. 3, p. 435–451.
Li, H.Y., Mao, J.W., Sun, Y.L., Zou, X.Q., He, H.L., and Du, A.D., 1996, Re-Os isotopic chronology of molybdenites in the Shizhuyuan polymetallic tungsten deposit, Southern Hunan: Geological Review, v. 42, no. 3, p. 261–267 (in Chinese with English abstract).
Li, X.H., Liu, D.Y., Sun, M., Li, W.X., Liang, X.R., and Liu, Y., 2004, Precise Sm-Nd and U-Pb isotopic dating of the supergiant Shizhuyuan polymetallic deposit and its host granite, SE China: Geological Magazine, v. 141, no. 2, p. 225–231.
Li, Z.L., Hu, R.Z., Peng, J.T., Bi, X.W., and Li, X.M., 2006., Helium isotope geochemistry of ore-forming fluids from the Furong tin orefield in Hunan Province, China: Resource Geology, v. 56, no. 1, p. 9–15.
Lippolt, H.J., and Weigel, E., 1988, ^{4}He diffusion in ^{40}Ar-retentive minerals: Geochimica et Cosmochimica Acta, v. 52, no. 6, p. 1449–1458.
Liu, Y.M., Wang, C.L., Xu, Y.Z., and Lu, H.Z., 1995, Metallization and metallogenetic conditions of Shizhuyuan ultra-large tungsten deposit: Hunan Geology, v. 14, no. 4, p. 211–219 (in Chinese with English abstract).
Lu, H.Z., Liu, Y.M., Wang, C.L., Xu, Y.Z., and Li, H.Q., 2003, Mineralization and Fluid inclusion study of the Shizhuyuan W-Sn-Bi-Mo-F skarn deposit, Hunan Province, China: Economic Geology, v. 98, p. 955–974.
Ma, T.Q., Wu, G.Y., Jia, B.H., Bo, D.Y., Wang, X.H., and Chen, B.H., 2005, Middle-Late Jurassic granite magma-mixing in the middle segment of the Nanling Mountains, South China: Evidence from mafic microgranular enclaves: Geological Bulletin of China, v. 24, no. 6, p. 506–512 (in Chinese with English Abstract).
Mamyin, B.A., and Tolstikhin, I.N., 1984, Helium isotopes in nature: Amsterdam, Elsevier Publishing Company, p. 1–273.
Mao, J.W., and Li, H.Y., 1995, Evolution of the Qianlishan granite stock and its relation to the Shizhuyuan polymetallic tungsten deposit: International Geology Review, v. 37, no. 1, p. 63–80.
Mao, J.W., Li, H.Y., Hidehiko, S., Louis, R., and Bernard, G., 1996, Geology and metallogeny of the Shizhuyuan Skarn-Greisen deposit, Hunan Province, China: International Geology Review, v. 38, no. 11, p. 1020–1039.
Mao, J.W., Li, H.Y., and Pei, R.F., 1995, Nd-Sr isotopic and petrogenetic studies of the Qianlishan granite stock, Hunan province: Mineral Deposits, v. 14, no. 3. p. 12–25.
Mao, J.W., Li, H.Y., Song, X.X., Rui, B., Xu, Y.Z., Wang, D.H., Lan, X.M., and Zhang, J.K., 1998, Geology and geochemistry of the Shizhuyuan W-Sn-Mo-Bi polymetallic deposit, Hunan, China: Beijing, Geological Publishing House, p. 1–215 (in Chinese with English abstract).
Mao, J.W., Li, H.Y., Wang, P.A., Guy, B., Perrin, M., and Raimbaull, L., 1994, Manganoan skarn in the Shizhuyuan polymetallic tungsten deposit, Hunan province: Mineral Deposits, v. 13, no. 1, p. 38–47 (in Chinese with English abstract).
McDdougall, I., and Harrison, T.M., 1988, Geochronology and thermochronology by the ^{40}Ar-^{39}Ar Method: New York, Oxford University Press, p. 1–269.

Patterson, D.B., Honda, M., and McDougall, I., 1994, Noble gases in mafic phenocrysts and xenoliths from New Zealand: Geochimica et Cosmochimica Acta, v. 58, no. 20, p. 4411–4428.

Peng, J.T., Zhou, M.F., Hu, R.Z., Shen, N.P., Yuan, S.D., Bi, X.W., Du, A.D., and Qu, W.J., 2006, Precise molybdenite Re-Os and mica Ar-Ar dating of the Mesozoic Yaogangxian tungsten deposit, central Nanling district, South China: Mineralium Deposita, v. 41, no. 7, p. 661–669.

Porcelli, D.R., O'Nions, R.K., Galer, S.G., Cohen, A.S., and Mattey, D.P., 1992, Isotopic relationships of volatile and lithophile trace elements in continental ultramafic xenoliths: Contributions to Mineralogy and Petrology, v. 110, no. 4, p. 528–538.

Reid, M.R., and Graham, D.W., 1996, Resolving lithospheric and sub-lithospheric contributions to helium isotope variations in basalts: Earth and Planetary Science Letters, v. 144, no. 1–2, p. 213–222.

Simmons, S.F., Sawkins, F.J., and Schlutter, D.J., 1987, Mantle-derived helium in two Peruvian hydrothermal ore deposits: Nature, v. 329, no. 6138, p. 429–432.

Smith, P.E., Evensen, N.M., York, D., Szatmari, P., and Oliveira, D.C., 2001, Single-crystal ^{40}Ar-^{39}Ar dating of pyrite: No fool's clock: Geology, v. 29, no. 5, p. 403–406.

Stuart, F.M., Burnard, P.G., Taylor, R.P., and Turner, G., 1995, Resolving mantle and crustal contributions to ancient hydrothermal fluids: He-Ar isotopes in fluid inclusions from DaeHwa W-Mo mineralisation, South Korea: Geochimica et Cosmochimica Acta, v. 59, no. 22, p. 4663–4673.

Stuart, F.M., Duckworth, R., Turner, G., and Schofield, P.F., 1994a. Helium and sulfur isotopes of sulfide minerals from Middle Valley, northern Juan de Fuca Ridge, *in* Mottl, M.J., Davis, E.E., Fisher, A.T., and Slack, J.F. eds., Proceedings of Ocean Drilling Program, volume 139, Scientific Results: College Station, Texas, Ocean Drilling Program, p. 387–392.

Stuart, F.M., Turner, G., Duckworth, R.C., and Fallick, A.E., 1994b, Helium isotopes as tracers of trapped hydrothermal fluids in ocean-floor sulfides: Geology, v. 22, no. 9, p. 823–826.

Sun, X.M., Xiong, D.X., Wang, S.W., Shi, G.Y., and Zhai, W., 2006, Noble gases isotopic composition of fluid inclusions in scheelites collected from Daping gold mine, Yunnan province, China, and its application for ore genesis: Acta Petrologica Sinica, v. 22, no. 3, p. 725–732 (in Chinese with English Abstract).

Tolstikhin, I.N., 1978, A review: Some recent advances in isotope geochemistry of light noble gases: *in* Alexander, E.C., Jr., and Ozima, M., eds., Terrestrial Noble Gases: Tokyo, Japan Scientific Press, p. 33–62.

Torgersen, T., Kennedy, B.M., and Hiyagon, H., 1988, Argon accumulation and the crustal degassing flux of ^{40}Ar in the Great Artesian Basin, Australia: Earth and Planetary Science Letters, v. 92, no. 1, p. 43–56.

Turner, G., Burnard, P., Ford, J.L., Gilmour, J.D., Lyon, I.C., and Stuart, F.M., 1993, Tracing fluid sources and interaction: Discussion: Physical Sciences and Engineering, v. 344, no. 1670, p. 127–140.

Wang, C.L., Luo, S.W., and Xu, Y.Z., 1987, Geology of the Shizhuyuan tungsten polymetallic deposit: Beijing, Geological Publishing House, p. 173 (in Chinese with English abstract).

Xu, K.Q., Sun, N., Wang, D.Z., Hu, S.X, Liu, Y.J., and Ji, S.Y., 1984, Petrogenesis and mineralization of south China granitoids, *in* Xu, K.Q., and Tu, G.Z., eds., Geology and Mineralization of Granitoids: Nanjing, Jiangsu Science and Technology Press, p. 1–20 (in Chinese).

Xu, W.X., Chen, M.Y., Xiao, M.H., and Zhou, Y.M., 2002, Isotope geochemistry of the Shizhuyuan W-Sn deposits from Hunan province: Geology and Mineral Resources of South China, no. 3, p. 78–84 (in Chinese with English abstract).

York, D., Masliwec, A., Kuybida, P., Hanes, J.E., Hall, C.M., Kenyon, W.J., Spooner, E.T.C., and Scott, S.D., 1982, ^{40}Ar/^{39}Ar dating of pyrite: Nature, v. 300, no. 4, p. 52–53.

Zhang, L.G., 1989, Stable isotope geochemistry of Qianlishan granites and tungsten-polymetallic deposits in Dongpo area, Hunan: Journal of Guilin College of Geology, v. 9, no. 3, p. 259–267 (in Chinese with English abstract).

Zhao, Y.M., 2004, Metallogenic law of main metallic ore deposit in China: Beijing, Geological Publishing House, p. 1–411 (in Chinese).

Zhao, Z.H., Bao, Z.W., Zhang, B.Y., and Xiong, X.L., 2001, Crust-mantle interaction and its contribution to the Shizhuyuan superlarge tungsten polymetallic mineralization: Science in China (D), v. 44, no. 3, p. 266–276.